Stochastic suppression of gene expression oscillations under intercell coupling

A. Koseska[1], A. Zaikin[1], J. García-Ojalvo[2], and J. Kurths[1]

[1]*Institut für Physik, Potsdam Universität, Am Neuen Palais 10, D-14469 Potsdam, Germany*
[2]*Departament de Física i Enginyeria Nuclear, Universitat Politècnica de Catalunya, Colom 11, E-08222 Terrassa, Spain*
(Dated: January 24, 2007)

This paper examines the dynamics of an ensemble of hysteresis-based genetic relaxation oscillators, focusing on the influence of noise and cell-to-cell coupling on the appearance of new dynamical regimes. In particular, we show that control of the coupling strength and noise can effectively change the dynamics of the system leading to behaviors such as clustering, synchronous and asynchronous oscillations, and suppression. Moreover, under certain conditions an optimal amount of noise can lead to increased order in the system. The results obtained are correlated with relevant biological processes that occur in living organisms.

I. INTRODUCTION

Many fundamental cellular processes are governed by genetic regulation programs based on gene-protein interactions. Since the complete structure and functionality of cellular processes remains still mainly unexplained, different mathematical models have been proposed in order to investigate cellular behavior, by using circuit and system theoretic models, including electrical circuits, Boolean networks, Bayesian networks, differential equations, Petri nets and weight matrices [1, 2].

Due to recent technological advances, the design of synthetic genetic networks has become possible [3, 4] and has been added to the list of theoretical and experimental tools for the study of gene-protein networks. This experimental progress has made genetic networks accessible to quantitative analysis [5, 6]. In certain cases, data obtained from synthetic-biology experiments have been proved consistent with the theoretical predictions of mathematical models, opening the gate for the understanding of gene regulatory networks.

As pointed out by Hasty et al. [6], there are two dominant reasons for the construction of synthetic genetic networks. First, simple networks represent a basic step towards the understanding of logical cellular control, whereby biological processes could be monitored or manipulated at the DNA level [7]. From the construction of simple switches or oscillators, one can envision the design of devices and software capable of performing elaborate functions in living cells [8, 9]. The second motivation for constructing networks of synthetic genetic oscillators is the notion of reduced complexity: decoupling a simple network from its native and often complex biological surrounding can lead to valuable information regarding evolutionary design principles [10], because both gene switches and oscillators are thought to be essential minimal modules in living organisms [11, 12]. Therefore, exploiting the behavior of networks constructed from synthetic genetic oscillators under different conditions, one could establish a solid theoretical background for designing genetic oscillator circuits. Such circuits could be further used in devices for sensing, computing, etc.

Experimental evidence shows that among most important factors affecting the performance of a cellular system within a living organism are noise [13, 14], inter-cellular communication [15], and population size [6, 13, 14]. The inherent stochasticity of biochemical processes, which depend on relatively infrequent molecular events involving small number of molecules, is an essential source of internal noise in biological systems. Additionally, fluctuations originating from the random variation of one or more externally-set control parameters act as external noise. Since the presence of noise in biological systems is inevitable, the consideration of its effects on the dynamics of gene networks is of course, very important.

Generally, intercellular communication is accomplished by transmitting individual states to neighboring cells via intercellular signals, and further integrating those signals to generate a global response at the levels of molecules, tissues, organs and the body. The ability to communicate among cells is an absolute requisite to ensure appropriate and robust coordination of cell activity at all levels of the organisms in an open environment [16].

Intercellular communication may have significant effects on the dynamics of cells. Cell-to-cell coupling in bacteria via quorum sensing, e.g., sometimes creates new dynamical regimes [15, 17, 18]. Most importantly, since quorum sensing dynamically interconnects proteins and genes between cells, the size of the population, meaning the number of cells interacting, can make a qualitative difference in the dynamics of the system.

The investigation of how the interplay between noise and intercell coupling may lead to qualitative changes in the dynamics of cells has not been pursued at an appropriate level so far. In this paper we try to shed light into this question, in the particular case of a coupled genetic relaxator model. The model used is a toggle switch driven via a hysteresis loop by intercell signaling. We first review previous studies on this model, highlighting the most important properties relevant for our work. Then we analyze the influence of a multiplicative noise source, as a means of controlling gene expression in the ensemble. We show that fluctuations can switch the dynam-

ics between synchronous and asynchronous oscillations, and lead to noise-induced suppression of oscillations in the ensemble, depending on the coupling strength. We find also that an optimal amount of noise can produce oscillations with a higher level of ordering. Finally, we present an overview of possible applications where these phenomena could be implemented.

II. MODEL EQUATIONS

Oscillatory behavior has been found in different specialized genetic networks, such as the ring oscillator or repressilator [3] and the relaxation oscillator [19]. In that context, a model of hysteresis-based relaxation genetic oscillators has recently been proposed [18]. This oscillator is constructed by combining two engineered gene networks, the toggle switch [4] and an intercell communication system, both of which have been previously implemented experimentally in *Escherichia coli*. These engineered gene networks are carried on multi-copy, self replicating plasmids that interfere minimally with the host cell. This allows one to consider the dynamics of the engineered network to be independent of the cell's natural regulatory circuitry. The toggle switch consists of two mutually repressing transcription factors. In its original version [4], these proteins are the lac repressor, encoded by the gene *lacI*, and a temperature sensitive variant of the λ cI repressor, encoded by the gene *cI857*. The synthesis of the two repressor proteins is regulated in such a way that the expression of the two genes (*cI857* and *lacI*) are mutually exclusive: the cell can be either in a state where the λ repressor is abundant and the *lac* repressor scarce (the *cI* on state) or in a state where the *lac* repressor is abundant and the λ repressor scarce (the *lacI* on state).

The presence of hysteresis in the toggle switch has been exploited to construct an oscillator network (Fig. 1), by coupling the toggle switch to a second module that autonomously drives cells through the hysteresis loop. This second module, intended to drive oscillations, involves components of the quorum-sensing system from *Vibrio fischeri*. Quorum-sensing enables cells to sense population density through a transcription factor protein *LuxR*, which acts as a transcriptional activator of genes expressed from the P_{lux} promoter when a small, organic molecule, the autoinducer (AI), binds to it. The AI is synthesized by the protein encoded by the gene *luxI*, and can diffuse across the cell membrane. The concentration of AI depends on that of LuxI, and can be controlled experimentally [18].

Following [18], we denote the *cI857* gene by v, the *lacI* gene by u, and the *luxI* gene by w. The time evolution of the concentrations of the three proteins for $i = 1, ..., N$ cells is governed by the dimensionless system:
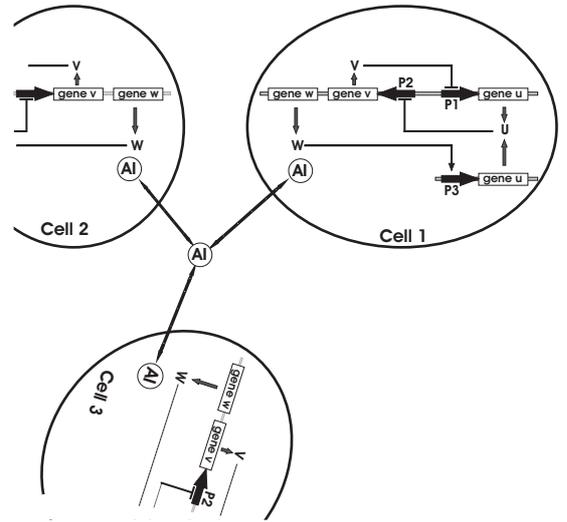
FIG. 1: Schematic diagram of the network of genetic relaxation oscillators.

$$\frac{du_i}{dt} = \alpha_1 f(v_i) - u_i + \alpha_3 h(\omega_i) \tag{1}$$

$$\frac{dv_i}{dt} = \alpha_2 e(u_i) - v_i \tag{2}$$

$$\frac{dw_i}{dt} = \varepsilon(\alpha_4 e(u_i) - w_i) + 2d(w_e - w_i) + g(w_i)\xi_i(t) \tag{3}$$

$$\frac{dw_e}{dt} = \frac{d_e}{N} \sum_{i=1}^{N} (w_i - w_e). \tag{4}$$

where w_e gives the time evolution of the extracellular AI concentration, and the regulatory functions are defined as:

$$f(v) = \frac{1}{1 + v^\beta}, \quad e(u) = \frac{1}{1 + u^\gamma}, \quad h(w) = \frac{w^\eta}{1 + w^\eta},$$

where β, γ and η are Hill coefficients.

The dimensionless parameters α_1 and α_2 regulate repressor in the toggle switch, α_3 determines the activation due to the autoinducer, and α_4 the repression of the autoinducer (for details, see [18]). The small parameter ε enables the appearance of relaxator dynamics. Two parameters that are of crucial importance in the analysis of this system are the coupling coefficients, d and d_e (intracellular and extracellular), defined as:

$$d = \frac{D}{2(1 + \delta_e/D_e)}, \quad d_e = D_e + \delta_e.$$

δ_e depends on the half-life of the proteins u and v, and on the effective first-order constant of removal of AI from the extracellular medium. D depends mainly on the diffusion coefficient, and D_e depends on both the diffusion coefficient and the ratio between the volume of the cells and the extracellular volume. Thus, the strength of coupling

among the cells can be varied by changing the diffusion properties of the membrane or the population density.

Finally, the last term in Eq. (3) models the contribution of random fluctuations, where $\xi_i(t)$ is a Gaussian white noise with zero mean and correlation $\langle \xi_i(t)\xi_j(t')\rangle = \sigma_a^2 \delta_{ij}\delta(t-t')$. The multiplicative noise is interpreted according to Stratonovich [20], which is the correct stochastic interpretation for a realistic noise with small temporal autocorrelation [21]. The noise term can incorporate both extrinsic and intrinsic stochastic sources. The former can be changed externally in experiments [22], what might result in large amplitude fluctuations [5, 22]. Physically, this type of noise might be generated by using an external field, e.g. electromagnetic field [5]. However, this externally variated noise remains uncorrelated for different cells in this case. We establish the function $g(w_i)$ by means of a simple approximation, consisting on assuming that the relative fluctuation scale is the inverse square-root of the concentration [23, 24],

$$\frac{g(w_i)}{w_i} \approx \frac{1}{\sqrt{w_i}}, \qquad (5)$$

which leads to

$$g(w_i) = \sqrt{w_i}. \qquad (6)$$

The proposed scaling is generic for many stochastic processes (e.g. Poisson process or birth/death processes) and provides a reasonable approximation to investigate the implications of fluctuations on biochemical regulatory circuits [23, 25].

III. DETERMINISTIC DYNAMICS

In gene regulation systems, many different time scales characterize the gene expression process. For instance, the transcription and translation processes generally evolve on a time scale much slower than that of phosphorylation, dimerization, or DNA binding of transcription factors. In the particular case of model (1)-(3), when the parameter ε is small ($\varepsilon \ll 1$), the evolution of the system splits into two well-separated time-scales. Due to this property, the system can produce relaxation oscillations. Moreover, varying the parameters α_1 and α_2, different regimes can be generated including oscillatory, bistable and monostable behaviors, as shown in the phase diagram plotted in Fig. 2.

Now let us illustrate the influence of cell-to-cell communication. We focus on the region where $d_e \gg d$, in order to avoid the frequency decrease described in [18]. Therefore, we are assuming that the population density is high, which experimentally would require some artificial conditions: the bacteria are locked in chambers under the flow of a liquid that supplies food in abundance. This is a model for more natural cluster formation phenomena, where the strong population density is of certain importance, as we will show with the model investigated.
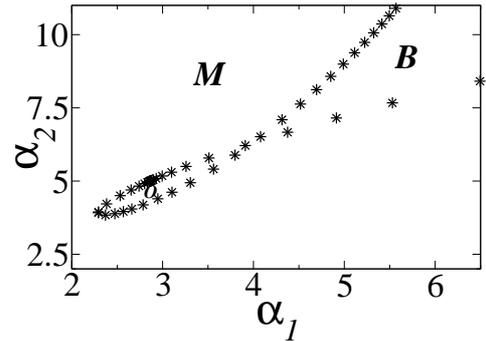
FIG. 2: Different dynamical regimes of a single oscillator: O - oscillatory regime, B - bistable regime, M - monostable regime. Parameters are $\sigma_a^2 = 0.0$, $\alpha_3 = 1.0$, $\alpha_4 = 4.0$, $\beta = \gamma = \eta = 2.0$, $\varepsilon = 0.01$.
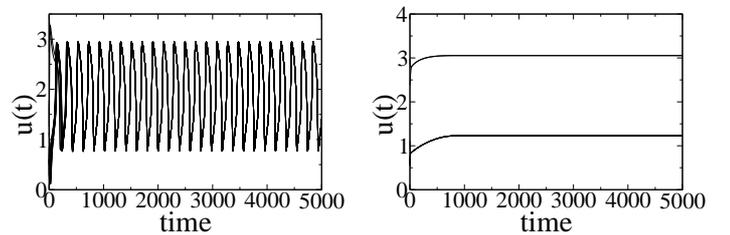
FIG. 3: Synchronous oscillations (left) and cluster solution (right). Parameters are those of Fig. 2, except $N = 20$, $\alpha_2 = 5.0$, $d_e = 1.0$ for both plots, $\alpha_1 = 3.0$, $d = 0.005$ in the left plot and $\alpha_1 = 2.9$, $\varepsilon = 0.05$ and $d = 0.3$ in the right plot.

In the oscillatory regime (region O in Fig. 2), macroscopic oscillations in protein concentration appear over the whole population, corresponding to synchronization between self-excited oscillators (Fig. 3, left). For larger values of the coupling strength ($d = 0.3$), two different regimes are possible (Fig. 4). This figure illustrates in detail the bifurcation structure of the full system when α_1 is varied, at a constant level of $\alpha_2 = 5$, as obtained with the software package XPPAUT [26]. First, there is a clustering solution (e.g. if $\alpha_1 = 2.9$), where oscillators are separated in two groups of cells exhibiting distinct steady states (Fig. 3, right). In the absence of coupling, in this region an isolated oscillator would be in the steady state. To increase the parameter region where this regime is observed, we have used $\varepsilon = 0.05$. However, for $\varepsilon = 0.01$ the bifurcation diagram looks qualitatively similar (not shown). Second, there is a parameter region (e.g. if $\alpha_1 = 3.0$) where two different regimes coexist: a regime of synchronous oscillations and a regime of oscillation death, where oscillators are grouped into two steady state clusters, like in a clustering regime just described. The difference is that in this parameter region, an isolated oscillator would be in the oscillatory state in the absence of cell-to-cell coupling.
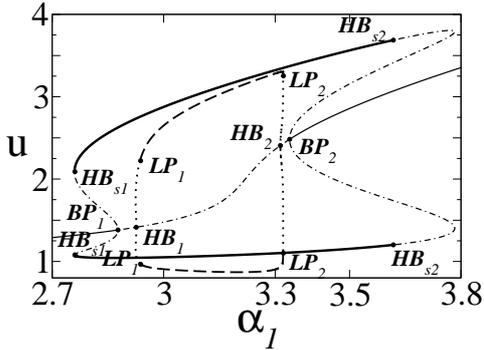
FIG. 4: Bifurcation diagram obtained by varying α_1, when the value of α_2 is kept fixed ($\alpha_2 = 5$). Other parameters are: $\alpha_3 = 1.0$, $\alpha_4 = 4.0$, $\beta = \gamma = \eta = 2.0$, $\varepsilon = 0.05$, $d = 0.3$ and $d_e = 1$. Thin solid lines represent stable steady states, dash-dotted lines correspond to unstable steady states, dashed lines represent stable limit cycles, dotted lines denote unstable limit cycles, and thick solid lines represent a situation with two stable clusters. Note that the Hopf bifurcation point HB_1 separates a region where the clustering state is a global attractor from another one in which that solution coexists with stable in-phase oscillations.

The regime of synchronous oscillations exists for a non-zero, but weak, coupling strength ($0 < d \ll 1$), where the AI is able to synchronize the oscillations over the entire population. The clustering or oscillation death regime occurs for larger coupling strengths and is characterized, as described above, by two clusters of silent oscillators producing constant protein levels.

IV. STOCHASTIC EFFECTS

The biochemical processes of transcription and translation depend on the number of promoter sites and mRNA molecules. These numbers are typically small, and thus cells may experience large fluctuations, which are usually seen as a source of internal noise. Furthermore, noise can also originate externally, in the random variation of one or more of the externally-set control parameters [27].

Because it is unavoidable in biochemical systems, noise in gene expression has been subject of many scientific investigations recently. For example, McAdams and Arkin [28] proposed theoretically, and van Oudenaarden confirmed experimentally [29] that most of the noise in gene expression in prokaryotic cells arises during transcription. It has also been observed experimentally that the dominant source of gene regulation noise is extrinsic, both in prokaryotic [30] and in eukaryotic [31] cells. However, the question of how the cell functions reliably in the presence of noise is still open. Recent numerical studies show that noise can play an ordering role in biochemical systems [32]. We now present further evidence in that direction, in this case in a *multicellular* system.

Specifically, we analyze in what follows the influence of noise on the system of genetic relaxation oscillators described above, for both the regimes of clustering and synchronous oscillations. First we examine the important influence of noise in isolated oscillator, where oscillations are seen to be *suppressed* by fluctuations. Then we show that an increase of noise in the system results in a rich dynamical behavior and leads to qualitative changes in the oscillation behavior. We also compare the different dynamical regimes created in the system due to noise.

A. Noise-induced suppression in a single oscillator

Figure 5 shows the behavior of an isolated cell, initially in the oscillatory regime, for increasing values of the noise intensity. The numerical analysis of the system is carried on with the Heun integration method [33] with step size control, i.e. for small concentrations, the step size has been also decreased.
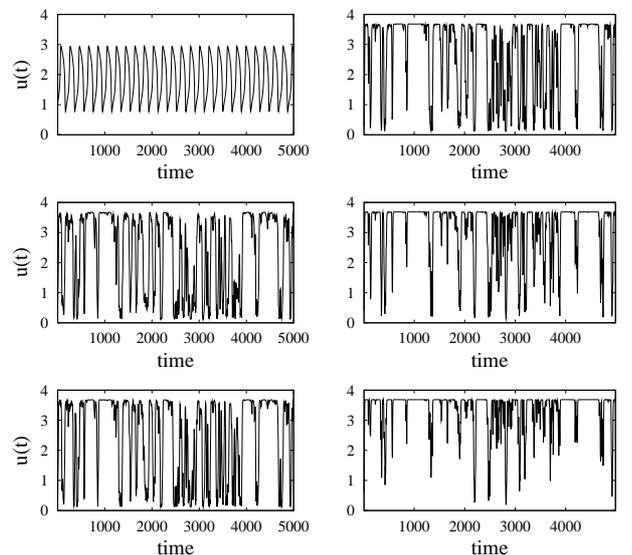
FIG. 5: Time series for one oscillator for different noise intensities. From top to bottom, and from left to right the noise increased: $\sigma_a^2 = 0$, 0.1, 0.2, 0.5, 1.5, 3.0. Other parameters as in Fig. 3, left.

We find that that the increasing noise shifts the dynamics of the system from regular (top left plot) to irregular (middle left plot) oscillations, while large enough noise levels suppress the oscillations (bottom right plot).

The effect of noise-induced suppression of oscillations can be explained by taking into account that, when the amplitude of fluctuations in the production rate of w_i [Eq. (3)] becomes sufficiently large, the protein level of w itself eventually reaches high levels, and when that happens the term $h(w) = \frac{w^\eta}{1+w^\eta}$ in Eq. (1) saturates ($h(w) \to 1$). This allows a simplification of this case, such that the system is governed only by the first two

equations of the original model (1)-(4):

$$\frac{du_i}{dt} = \alpha_1 f(v_i) - u_i + \alpha_3$$
$$\frac{dv_i}{dt} = \alpha_2 g(u_i) - v_i$$

To find the stationary solutions of the system in this case, we set $\frac{du_i}{dt} = 0$ and $\frac{dv_i}{dt} = 0$. The equilibrium states can be found as zeroes of the following function:

$$F(u) = u - \frac{\alpha_1(1 + u^\gamma)^\beta}{\alpha_2^\beta + (1 + u^\gamma)^\beta} - \alpha_3 , \qquad (7)$$

the solution of which can be obtained graphically by plotting $F(u)$ vs. u, as shown in Fig. 6. The plot reveals that
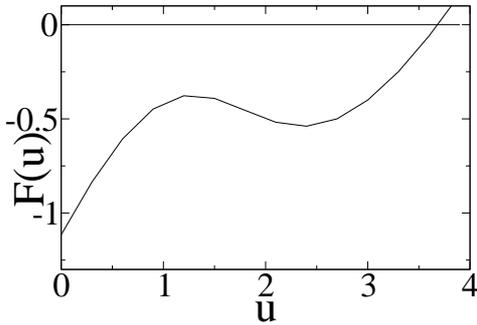
FIG. 6: Graphical solution of the equation (7).

the system has a single steady state at high u, which happens to be stable. This indicates that oscillations are suppressed for high enough noise intensities.

Note that even though the noise intensities required for suppression are somewhat large, they are experimentally sensible, and furthermore they do not lead to unrealistic situations (such as negative values of the fields) for small concentrations, since we have chosen $g(w_i)$ in such a way that the amplitude of the fluctuations decreases for decreasing protein levels, and are zero at $w_i = 0$. It is well known that such a multiplicative noise term, when interpreted according Stratonovich, produces a systematic effect due to its mean being non-zero, what is know as the Stratonovich drift [21]. It might seem that the suppression described above is due to that drift term. However, the phenomenon persists even when the noise is purely additive ($g(w_i) = 1$, results not shown). This is an unrealistic situation where the AI concentration can become negative, and as such is not considered in this paper. However, the persistence of suppression in this case shows that the phenomenon just requires that the AI concentration becomes large intermittently.

It is known that simulations of Langevin equations along the same lines as those considered here correlate well with a discrete description of the biochemical processes involved using, e.g. the Gillespie approach [34].

However, we have checked with a simplified approach that the results discussed above are also obtained within a discrete description. To that end, we rewrote the stochastic model (1)-(4) in the Ito form (i.e. introducing explicitly the Stratonovich drift term) [20] and applied the Gillespie algorithm to the resulting model [35, 36]. With these assumptions, a typical time series generated with the Gillespie algorithm is shown in the right plot of Fig. 7, and is seen to compare favorably with the simulations of the Langevin equations (left plot in the Figure).
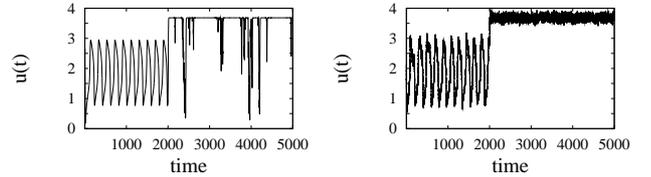
FIG. 7: Time-series for a single gene circuit in the oscillating regime. The noise is switched on at $t = 2000$. Left: simulations of the Langevin stochastic differential equations (1)-(4). Right: simulations using the Gillespie algorithm applied to the corresponding discrete system (see text). Parameters are as in Fig. 3, left.

B. Noise in the stable synchronous regime

Next, we analyze the influence of noise on the system in presence of cell-to-cell communication. As a reference, we first consider the behavior of the system in the absence of noise. When the coupling strength is weak ($0 < d \ll 1$), the AI is present at a relatively small concentration and is able to synchronize the oscillations over the entire population. In our model, the AI plays a double role: inside the cell it is used to switch the production of the two proteins of the switch, when their concentration levels are high enough and the conditions for switching are fulfilled; additionally, it is used to synchronize the oscillations among different cells, as we mentioned.

When noise is present in the system, it produces fluctuations in the AI concentration, which now disturbs the synchronous oscillations in the system. The behavior of different cells is affected and as a result, asynchronous oscillations of the protein concentrations occur over the entire population (see Fig. 8, left plots). If the noise is increased even further, the fluctuations in the AI (both extracellular and intracellular) are high, and the system behaves as if a large AI concentration is present. In that case, genetic switching is not established and a stable production of the two proteins occurs. Due to the large fluctuations of the AI concentration, however, the system will have only one stable solution (explanation given in section IV A), which will be populated by all oscillators present in the system. Since there are no oscillations for large noise intensities, we refer to this effect as noise-induced suppression of oscillations (see Fig. 8, right plots).
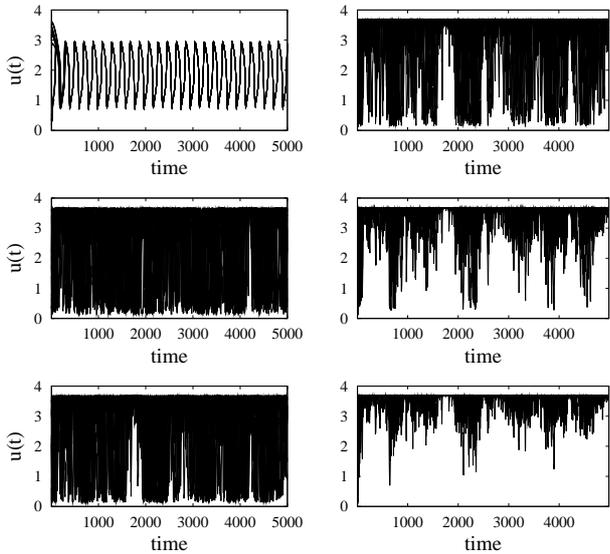
FIG. 8: Dynamics of the system for different noise intensities. From top to bottom, and left to right: $\sigma_a^2 = 0, 0.1, 0.2, 0.5, 1.5, 3.0$. Other parameters as in Fig. 3, left.

The effect of noise-induced suppression resembles that of stochastic focusing [37], since suppression is enhanced by the high nonlinearity of the function $h(w)$. As pointed out in [37], stochastic focusing is similar to the effect of stochastic resonance, because more noise leads to an increased order in the system. A similar statement could be made for noise-induced suppression, where larger noise intensities also lead to ordering of the oscillators in one cluster.

In order to describe quantitatively the different dynamical regimes that emerge in the presence of the noise, we introduce the following order parameters:

$$ j = \frac{N_j}{NT}, \qquad f = \left\langle \frac{N_u}{N} \right\rangle \qquad (8) $$

where N is the total number of cells, N_j the number of jumps over a predefined threshold (we choose $u = 2$ in the present case), N_u is the number of cells above this threshold, T is the total time, and $\langle \cdot \rangle$ denotes time averaging. Consequently, j measures the number of jumps above a threshold, averaged over the total number of oscillators and the integration time, whereas f is the fraction of cells above the threshold.

The order parameter j (Fig. 9, left) has a well defined value for zero noise intensity (giving the number of jumps over threshold for the stable synchronous solution). As explained above, for moderate noise intensities the synchronous solution is disrupted, engaging the system into the regime of asynchronous oscillations. This corresponds to a constant increase of j, until a maximum is reached for a certain noise intensity. Further increase of the noise intensity affects the dynamics of the AI up to the point where fluctuations in the system are large enough to quench the oscillations, leading
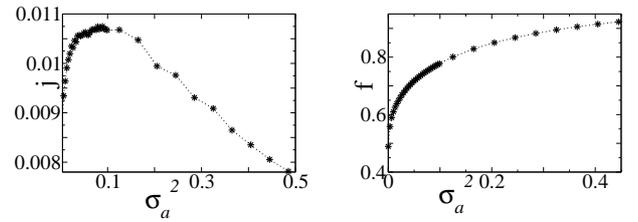
FIG. 9: Order parameters j (left) and f (right) vs. noise intensity (σ_a^2) for the stable synchronous solution.

to noise-induced suppression (characterized by a value of j decreasing towards 0). The other order parameter, f, follows the transition of the oscillators in the system from the case where they oscillate to the point where they all move to the upper stable state, giving the noise intensity when the oscillations in the system will be suppressed (Fig. 9, right). Important conclusions about the order in the system can be revealed by estimating the coherence of the oscillations. Since the system undergoes noise-induced jumps, its time evolution for different noise intensities can be viewed as a sequence of pulses of duration t_p. In order to characterize the order quantitatively, we compute the variability of the pulse duration (oscillation period) via the coefficient of variation (or normalized standard deviation), $R_p = \frac{\sqrt{\mathrm{var}(t_p)}}{t_p}$ [38], where $\mathrm{var}(t_p)$ denotes the variance. In the context of coherence resonance, this parameter characterizes the temporal coherence or periodicity of oscillations. Smaller values of R_p mean larger coherence. In the present case, as shown in Fig. 10, the dependence of this quantity on the noise intensity shows a continuous growth, meaning that noise destroys order in a monotonic way.
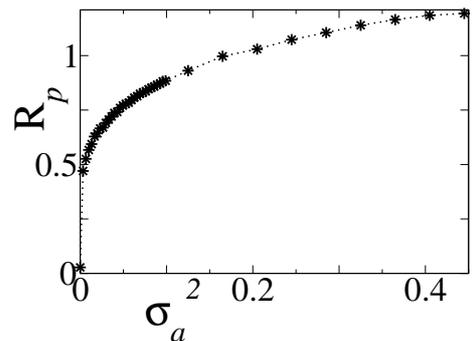
FIG. 10: Coherence parameter of the system. The coherence is maximal ($R_p = 0$) for $\sigma_a^2 = 0$. Increase of noise intensity in the system destroys the synchronous solution, which results in asynchronous oscillations (value of R_p is increased).

Hasty and Collins have suggested that noise is important in gene expression systems [39] because it can be used by an organism in deciding between alternative

states, such as a particular developmental pathway. The asynchronous oscillations of the population that we observe in the presence of noise can be viewed as a heterogeneity in the population, where the population creates many different possible pathways for its survival in the future. The conditions in the surrounding environment will possibly influence the future state of the system. This implies that real systems might use the noise-"created" heterogeneity as a method of adaptation to different survival conditions.

C. Noise in the clustering regime

Similarly to the case of stable synchronous oscillations, noise also affects the dynamics of the system when the oscillators are initially distributed between two stable steady state clusters. Again, the system is observed to undergo noise-induced jumps, with apparent coherent behavior for a given noise intensity, in transit to a state where all of the oscillations are suppressed and the oscillators populate the upper steady cluster.

Due to the structural properties of the genetic network under investigation, when the coupling strength is large enough (meaning that the concentration of the AI is large enough to entrain the oscillations in the system), constant concentrations of the proteins are obtained, and different oscillators will be distributed among these states (Fig. 11, top left). When small noise is present in this system, it causes fluctuations in the AI concentration, affecting the dynamics of the protein production. Gene expression is now able to switch between both states, i.e. undergoes noise-induced jumps, which lead to asynchronous oscillations of the protein concentrations in the different cells (Fig. 11, bottom left). If noise is increased further, and similarly to the previous section, the fluctuations of the AI concentration become large enough to be able to quench the oscillations. Only the upper state is stable under these conditions. Therefore, all the oscillators will shift to this state, and noise-induced suppression can be observed once more (Fig. 11, right plots).

We can use the order parameters defined in Eq. (8) to determine the noise intensity needed for suppression in this case, as well as the noise intensity at which all of the oscillators in the system shift to the upper stable state. By definition, the order parameter j is zero when the noise is absent, since the oscillations are quenched due to the coupling strength. When noise starts to affect the system, its dynamics changes as explained above. Asynchronous oscillations are now born in the system, characterized by an increase in the number of jumps, and consequently an increase of j (Fig. 12, left). When the noise intensity is large enough, the value of j starts to decrease towards zero, where noise induced-suppression is observed. The shift of the different oscillators to the upper stable state is expressed by the behavior of f with respect to the noise intensity (Fig. 12, right).

The coherence parameter R_p reveals another interest-
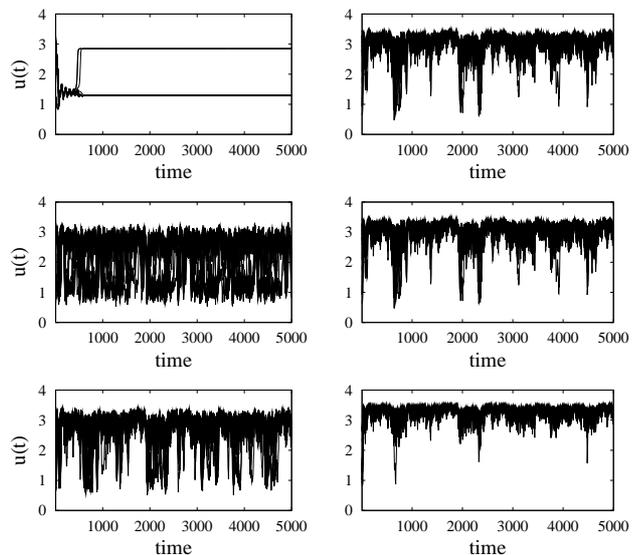
FIG. 11: Dynamics of the system for different noise intensities. From top to bottom and from left to right: $\sigma_a^2 = 0, 0.1, 0.2, 0.3, 0.4, 0.5$. Other parameters as in Fig. 3, right.
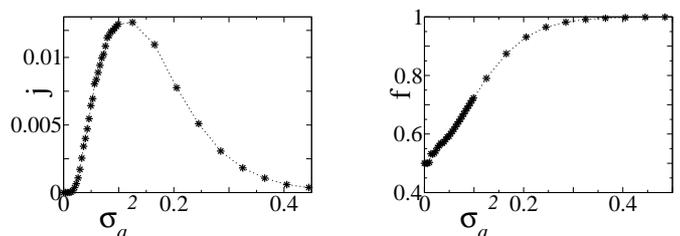
FIG. 12: Order parameters j (left) and f (right) vs. noise intensity (σ_a^2) for the oscillation death regime.

ing property of the system in this case. As shown in the left panel of Fig. 13, for small and large noise intensities, noise-excited oscillations appear to be rather irregular, while for moderate noise intensities, relatively coherent oscillations are observed. This implies that if the noise level present in the system is of moderate intensity, noise-induced jumps in the system are relatively periodic. This is an example of coherence resonance [38].
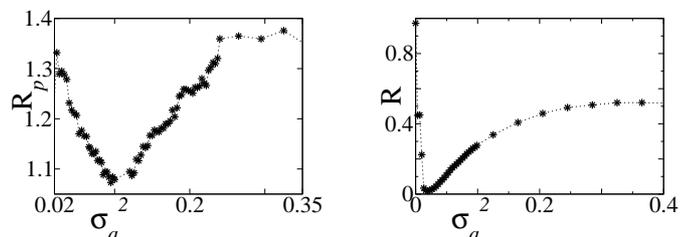
FIG. 13: Left: Coherence parameter R_p for increasing noise intensity; Right: Synchronization level R vs. noise intensity.

In order to quantify the level of synchronization in the system, we use the following order parameter [17]:

$$R = \frac{\langle M^2 \rangle - \langle M \rangle^2}{\overline{\langle u_i^2 \rangle - \langle u_i \rangle^2}} , \qquad (9)$$

where $\langle \cdots \rangle$ denotes time average, $\overline{\cdots}$ indicates average over all cells, and we have defined the mean field $M(t) = (1/N) \sum_{i=0}^{N} u_i(t)$, which in the synchronized case will be similar to each one of the local signals $u_i(t)$. On the other hand, when the oscillators are not synchronized, the individual signals $u_i(t)$ are completely out of step with respect to each other, and their sum will be averaged out to an approximately constant value at all times. Therefore, the order parameter R is defined as the ratio of the standard deviation of the time series of $M(t)$ to the standard deviation of $u_i(t)$ averaged over i. In this way, in the unsynchronized regime $R \approx 0$, whereas $R \approx 1$ refers to the synchronized case.

Computing the order parameter R for this case, we can identify a synchronization transition occurring as the noise level is changed. The right panel of Fig. 13 shows that for $\sigma_a^2 > 0.02$ (where coherence resonance was observed) the value of R is increased, corresponding to the regime where the oscillators are most ordered, i.e synchronized in the presence of noise. This correspond also to the decrease of the coherence parameter, i.e. improvement of the periodicity (Fig. 13 left). The value of R does not approach exactly 1 because in the presence of noise synchronization is not complete. For stronger noise intensities ($\sigma_a^2 > 0.4$), the oscillations are continously suppressed, and the oscillators populate the upper stable steady state. Moreover, an increase of the synchronization level is also characterized by an increase of noise-induced jumps, as measured by the parameter j. Note also that in the clustering regime, one needs much less noise to obtain suppression than in the oscillatory regime. This can be explained by the fact that the state towards which the oscillation quench already exists.

As mentioned above, the question of how cells function reliably in the presence of noise is still open. The fact that order in the population of synthetic genetic oscillators is optimal for moderate noise intensities clearly implies that noise in real systems plays a constructive role, leading to more order in the dynamics.

D. Comparing noise effects for different coupling levels

We have seen that a large enough noise suppresses oscillations and stabilizes the dynamics of the genetic relaxation oscillators, both when the deterministic behavior exhibits synchronous oscillations and in the regime of clustering. In spite of the similar limiting behavior for large noise, the stochastic effects differ for different coupling. In particular, for large coupling (clustering or oscillation death regime in the absence of fluctuations)

noise has a much stronger influence, as revealed by the average number of jumps j shown in the left panel of Fig. 14. The plot reveals that the number of jumps is higher when the system departs, in the absence of noise, from the clustering regime than from the synchronous oscillation regime. This can be due to the fact that in the former regime, each of the cells behaves as a bistable system driven by noise, whereas in the latter case oscillations are already present in the system, and noise is not inducing many new jumps. In its turn, for the regime of coexistence of synchronous oscillations with oscillation death, the number of jumps is always smaller. Note also that in the regimes that exhibit cluster formation (both with and without coexistence) one needs much smaller noise intensity for the suppression than in the oscillatory regime. This can be also vizualised in the left panel of Fig. 14. Again the oscillatory/oscillation death regime is suppressed faster than the two other regimes.
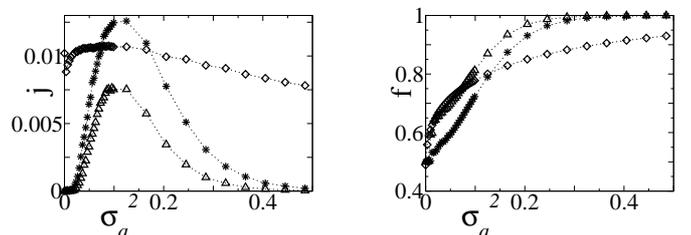
FIG. 14: Average number of jumps j (left) and suppression parameter j (right) versus noise intensity for three different coupling regimes. Diamonds correspond to the synchronous oscillation regime (low coupling $d = 0.005$, $\alpha_1 = 3$ and $\epsilon = 0.01$.), stars to the clustering regime (large coupling $d = 0.3$, $\alpha_1 = 2.9$ and $\epsilon = 0.05$.) and triangles to the co-existing oscillation death and oscillatory regimes (large coupling $d = 0.3$, $\alpha_1 = 3$ and $\epsilon = 0.05$.). Other parameters are: $\alpha_2 = 5, \alpha_3 = 1, \alpha_4 = 4$, and $\beta = \gamma = \eta = 2$.

The transition through the various regimes occurring under the influence of noise can be also represented as follows. In Fig. 15, the x-axis represents time, while the different oscillators are displayed along the y-axis. The value of u is shown in color code for each oscillator and each time instant. In both plots of Fig. 15 noise is increased in two steps, at times $t = 2000$ and $t = 4000$. The top plot corresponds to a situation where the system exhibits, in the absence of noise ($t < 2000$), synchronous oscillations in protein concentration. For the noise intensity $\sigma_a^2 = 0.12$ ($2000 < t < 4000$), asynchronous oscillations are present, while for the noise intensity $\sigma_a^2 = 1.0$ ($t > 4000$), noise induced-suppression is observed. On the other hand, the bottom plot of Fig. 15 corresponds to a regime in which for zero noise ($t < 2000$) a clustering regime occurs, and the oscillators populate one of two stable states. For the noise intensity $\sigma_a^2 = 0.12$ ($2000 < t < 4000$), asynchronous oscillations are created, while for the strong noise intensity $\sigma_a^2 = 0.5$, noise induced suppression is observed ($t > 4000$). Comparing
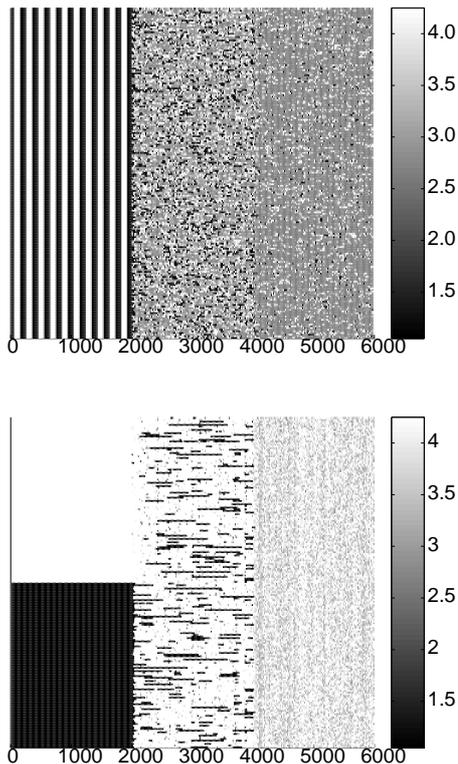
FIG. 15: Overview of the dynamical evolution of the coupled oscillators. Noise is increased step-wise at $t = 2000$ and $t = 4000$. The top panel corresponds to the regime of synchronous oscillations, the bottom panel to the clustering regime. The noise intensity is 0.0, 0.12, and 1.0 (top) and 0.0, 0.12, and 0.5 (bottom). The time series are plotted for a system of 200 relaxation oscillators, each of them denoted by the horizontal line, with color encoding corresponding the color scale shown on the right. On the plot the horizontal lines are very close so that they are indistinguishable. Note that without cell-to-cell communication, the single oscillator would be in a simple oscillating regime.

upper and bottom plots again one can see that different noise intensities (larger for in-phase regime) are needed for the full suppression when starting from in-phase or clustering regime (see also Fig. 14).

It is also worth mentioning at this point that if the noise acts upon the fast variables of the system (u, v), the effect of noise induced suppression is not observed (results not shown in the paper). Further investigation is needed of that case.

V. SUMMARY AND OUTLOOK

We have studied effects of noise and population size on an ensemble of genetic relaxation oscillators. It is well known that noise cannot be avoided in biochemical systems, causing many experimental issues on the behavior of such genetic oscillators. We have shown, however, that naturally occurring noise can be exploited to control the dynamics of the system, switching between synchronous and asynchronous oscillations and oscillation suppression.

The control over gene expression in ensembles of coupled synthetic genetic oscillators opens new approaches in biotechnology, enabling scientists to develop a new era of devices for sensing, computing, drug production, etc. This new approach of investigation through the construction of synthetic genetic networks implemented in real cells could allow the manipulation of biological processes at a genetic level and create more complete models of the behavior of natural systems.

From a different perspective, an adequate control of the performance of synthetic genetic oscillators or switches might enable the construction of integrated biological circuits capable of performing increasingly elaborate functions, with data-processing and storage capabilities, which would gradually change the direction of computing. If constructed, these new devices will allow more cost-efficient devices that would outweigh present memory units, for example. Synthetic genes, encoded into the DNA, might be "downloaded" into a cell, creating in that way a nano-robot, which could be used for *in vivo* biosensing, autonomous synthesis of complex biomaterial, execution of programmed cell death, or interfacing with microelectronic circuits by transducing biochemical events to and from electronics.

[1] H. McAdams and L. Shapiro, Science **269** (1995).
[2] L. Chen and K. Aihara, IEEE Trans. Circ. Syst. I **49**, 1429 (2002).
[3] M. B. Elowitz and S. Leibler, Nature **403**, 335 (2000).
[4] T. S. Gardner, C. R. Cantor, and J. J. Collins, Nature **403**, 339 (2000).
[5] J. Hasty, J. Pradines, M. Dolnik, and J. J. Collins, Proc. Natl. Acad. Sci. USA **97**, 2075 (2000).
[6] J. Hasty, J. J. Collins, F. Isaacs, M. Dolnik, and D. McMillen, Chaos **11**, 207 (2001).

[7] W. Chen, P. Kallilo, and J. E. Bailey, Genetics **130** (1993).

[8] D. Bray, Nature **376**, 307 (1995).

[9] R. Weiss and T. Knight, DNA6: 6th International Meeting on DNA Based Computers (Leiden, the Netherlands) (2000).

[10] N. Barkai and S. Liebler, Nature **403**, 267 (2000).

[11] T. Kobayashi, L. Chen, and K. Aihara, J. Theor. Biol. **221** (2003).

[12] G. Süel, J. Garcia-Ojalvo, L. Liberman, and M. Elowitz, Nature **440**, 545 (2006).

[13] M. B. Elowitz, A. J. Levine, E. D. Siggia, and P. S. Swain, Science **297**, 1183 (2002).

[14] P. S. Swain, M. B. Elowitz, and E. D. Siggia, Proc. Natl. Acad. Sci. USA **99**, 12795 (2002).

[15] D. McMillen, N. Kopell, J. Hasty, and J. J. Collins, Proc. Natl. Acad. Sci. USA **99**, 679 (2002).

[16] R. Wang and L. Chen, J. Biol. Rhyth. **20**, 257 (2005).

[17] J. Garcia-Ojalvo, M. Elowitz, and S. Strogatz, Proc. Natl. Acad. Sci. USA **101**, 10955 (2004).

[18] A. Kuznetsov, M. Kern, and N. Kopell, SIAM J. Applied Math. **65**, 392 (2005).

[19] N. Atkinson, M. Savagean, J. Myers, and A. Ninfa, Cell **113**, 597 (2003).

[20] C. Gardiner, *Handbook of Stochastic Methods* (Springer, Berlin, 1985).

[21] J. García-Ojalvo and J. M. Sancho, *Noise in Spatially Extended Systems* (Springer, New York, 1999).

[22] W. J. Blake, M. Kaern, C. R. Cantor, and J. J. Collins, Nature **422**, 633 (2003).

[23] R. Steuer, Journal of Theoretical Biology **228**, 293 (2004).

[24] T. Kepler and T. Elston, Biophys. J. **81** (2001).

[25] N. van Kampen, *Stochastic Processes in Physics and Chemistry* (North-Holland, Amsterdam, 1981).

[26] B. Ermentrout, *Simulating, Analyzing, and Animating Dynamical Systems: A Guide to Xppaut for Researchers and Students (Software, Environments, Tools)* (SIAM Press, 2002).

[27] J. M. Raser and E. K. O'Shea, Science **309**, 2010 (2005).

[28] H. H. McAdams and A. Arkin, Proc. Natl. Acad. Sci. USA **94**, 814 (1997).

[29] E. M. Ozbudak, M. Thattai, J. Kurtser, A. D. Grossman, and A. van Oudenaarden, Nature Genetics **31**, 69 (2002).

[30] N. Rosenfeld, J. W. Young, U. Alon, P. S. Swain, and M. B. Elowitz, Science **307**, 1962 (2005).

[31] J. M. Raser and E. K. O'Shea, Science **304**, 1811 (2004).

[32] R. Steuer, C. Zhou, and J. Kurths, Biosystems **72**, 241 (2003).

[33] P. Kloeden and E. Platen, *Numerical Solution of Stochastic Differential Equations* (Springer-Verlag, Berlin, 1992).

[34] Z. Wang, Z. Hou, and H. Xin, Chemical Physics Letters **401** (2005).

[35] D. Gillespie, J. Comput. Phys. **22**, 403 (1976).

[36] D. Adalsteinsson, D. McMillen, and T. Elston, BMC Bioinformatics pp. 5–24 (2004).

[37] J. Paulsson, O. G. Berg, and M. Ehrenberg, Proc. Natl. Acad. Sci. USA **97**, 7148 (2000).

[38] A. Pikovsky and J. Kurths, Phys. Rev. Lett. **78**, 775 (1997).

[39] J. Hasty and J. J. Collins, Nature Genetics **31**, 13 (2004).